Fast equilibrium switch of a micro mechanical oscillator

Anne Le Cunuder,[1] Ignacio A. Martínez,[1] Artyom Petrosyan,[1] David Guéry-Odelin,[2] Emmanuel Trizac,[3] and Sergio Ciliberto[1,a)]
[1]*Université de Lyon, CNRS, Laboratoire de Physique de l'École Normale Supérieure, UMR5672, 46 Allée d'Italie, 69364 Lyon, France*
[2]*Laboratoire de Collisions Agrégats Réactivité, CNRS UMR 5589, IRSAMC, Toulouse, France*
[3]*LPTMS, CNRS, Univ. Paris-Sud, Université Paris-Saclay, 91405 Orsay, France*

(Received 6 June 2016; accepted 2 September 2016; published online 16 September 2016)

We demonstrate an accurate method to control the motion of a micromechanical oscillator in contact with a thermal bath. The experiment is carried out on the cantilever tip of an atomic force microscope. Applying an appropriate time dependent external force, we decrease the time necessary to reach equilibrium by two orders of magnitude compared to the intrinsic equilibration time. Finally, we analyze the energetic cost of such a fast equilibration, by measuring with $k_B\,T$ accuracy the energy exchanges along the process. *Published by AIP Publishing.*
[http://dx.doi.org/10.1063/1.4962825]

The last decade witnessed spectacular advances in the fabrication and control of high-quality micromechanical oscillators. They are nowadays widely used in applications including timing, synchronization, high precision sensing of force, acceleration and mass. They even provide an interesting connection between quantum resources dedicated to quantum state manipulations and resources for transmitting quantum states.[1–3]

Most applications involve micromechanical oscillators in the underdamped regime and in contact with a thermal bath. In the present letter, we implement a generic method to speed up the transition between the two equilibrium states of such a micromechanical oscillator in the limit where the relevant description is that provided by the 1D underdamped harmonic oscillator in the presence of thermal noise. Such a system evolves towards a new equilibrium state by dissipating energy along an oscillating dynamics whose amplitude decreases with a relaxation time of $\tau = m/\gamma$, where m is the oscillator mass and γ the viscous coefficient, which depends on the surrounding medium and the probe geometry. The reduction of the duration time of the transient regime to an arbitrary time $t_f \ll \tau$ is an important issue for applications, such as Atomic Force Microscopy (AFM), which has become a pivotal tool in the experimental study of biological systems, material science, polymer physics, etc. Many experiments are done in gaseous media, which increases the quality factor and produces long transients. An arbitrary acceleration of the equilibration time of AFM cantilevers is the basis of the high speed AFM, and it has been achieved, in particular, using feedback techniques[4–6] or changing the viscoelastic behavior of the cantilevers.[7] Alternatively, it has been recently shown that, in the case of an overdamped system, fast relaxation can be obtained by using an appropriate driving force which remains efficient even in a very noisy environment. This result was obtained on a Brownian particle trapped by optical tweezers and the new equilibrium was reached 100 times faster than the natural equilibration time.[8] Here, we generalize this idea, referred to as Engineered Swift Equilibration (ESE), to the underdamped systems, using as micromechanical oscillator the cantilever tip of an atomic force microscope. We also measured directly the energy needed in the course of the transformation to accelerate the process. Our approach is therefore of the feed-forward type, and in that, it belongs to a category of techniques known in the engineering community as *input shaping*.[6,9]

Specifically, we propose an ESE protocol, which does not require any feedback and which is based only on a statistical analysis of the cantilever tip position $x(t)$, whose dynamics is described with a rather good accuracy by a second order Langevin equation

$$m\ddot{x} = -\gamma\dot{x} - \kappa x + F(t) + \zeta(t), \tag{1}$$

where κ is the stiffness of the system and F the external applied force. ζ is a white noise delta correlated in time: $\langle\zeta(t)\zeta(t')\rangle = 2\gamma k_B T\delta(t-t')$. The resonant frequency $\omega_o = \sqrt{\kappa/m}$ is the frequency of the first cantilever mode. The process that we want to speed up is the transition of the cantilever tip from an initial equilibrium position x_i to a new one x_f, obtained by applying a time dependent force $F(t)$.

In the case of an underdamped oscillator in the presence of thermal fluctuations, the equilibrium velocity and position probability distribution function (pdf) $\rho_{eq}(x,v,t)$ reads as $\rho_{eq}(x,v) = \frac{1}{Z}\exp\left[-\frac{\kappa x^2}{2k_BT} - \frac{Fx}{k_BT}\right]\exp\left[-\frac{mv^2}{2k_BT}\right]$, where κ, m, and T are fixed all along the protocol and Z is the partition function. Once a parameter is changed, for example, the external force F, the Kramers equation gives us the evolution of the pdf. By appropriately tuning the strength of F as a function of time, it is possible to force the system to equilibrate in a given time t_f. This is the spirit of the ESE protocols.

Specifically, in our ESE process (see supplementary material for an accurate derivation), the force evolves according to a polynomial equation in the normalized time $s = t/t_f$ as

$$\frac{F(s)}{\kappa\,x_f} = s^3(10 - 15s + 6s^2) + \frac{\gamma}{\kappa t_f}(30s^2 - 60s^3 + 30s^4) + \frac{m}{\kappa t_f^2}(60s - 180s^2 + 120s^3), \tag{2}$$

a)Electronic mail: sergio.ciliberto@ens-lyon.fr

with boundary conditions $F(t)=0$ for $t<0$ and $F(t)/\kappa = F_f/\kappa = x_f$ for $t>t_f$. Interestingly, the protocol dependence on the final position x_f is separable and keeps its shape under different traveling distances. Eq. (2) is factorized in that way to clearly show the three terms corresponding to the three different regimes determined by the values of t_f, i.e., $t_f \gg \gamma/\kappa$, $2\pi/\omega_o \leq t_f \leq \gamma/\kappa$, and $2\pi/\omega_o > t_f$. As demonstrated in the following, the system will reach the desired equilibrium state from its initial equilibrium state using this protocol and in the time interval t_f that we choose.

The sketch of the experimental setup is illustrated in Fig. 1(a). The oscillator under consideration is a silicon cantilever (size 500 μm × 30 μm × 2.7 μm, NanoAndMore) with a polystyrene sphere (Sigma-Aldrich, $R=75$ μm) glued on its tip. We will refer to this ensemble sphere-cantilever as the probe. The whole probe and the flat surface, facing the sphere, are coated with a 100 nm thick gold layer. The experiment is done in nitrogen atmosphere at room temperature $T=300$ K and pressure $p=1$ bar. Therefore, the viscosity is very low, which gives a completely underdamped dynamics. The surface-sphere distance d can be tuned using an electronically controlled piezostage (Piezo Jena). The position $x(t)$ of the cantilever tip is measured by a highly sensitive interferometer with subpicometer resolution and high speed acquisition $f_{\text{acq}}=200$ kHz.[10] The stiffness, viscosity, and mass are the intrinsic parameters of the oscillator and are calibrated using the Brownian motion of the thermally excited probe; in this specific case, $\kappa = (2.50\pm0.50)$N/m, $\gamma = (1.00\pm0.30)\times10^{-6}$ N s/m, and $m = (8.37\pm0.16)\times10^{-9}$ kg. Hence, the resonance of the first mode of the probe is $\omega_o = 17.3$ krad/s.

An attractive electrostatic interaction is generated by applying a voltage difference $V(t)$ between the surface and the sphere. The sphere-surface force can be written as

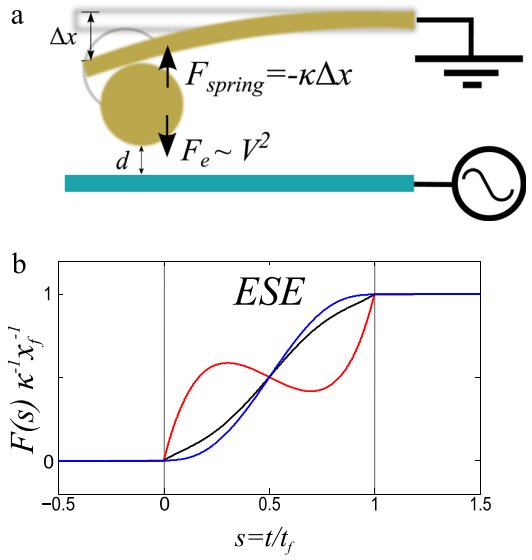

FIG. 1. (a) Sketch of the experimental setup. The cantilever-sphere system is connected to the ground, while the surface is connected to the signal generator. The external force is applied by the voltage difference between them. (b) Force ESE protocol for different final times $t_f=0.2$ ms (red), 0.5 ms (black), and 2 ms (blue) as a function of the normalized time $s=t/t_f$. If we reduce enough the protocol time, the inertial term of the protocol becomes dominant and yields a nonmonotonous force (see the red curve).

$F = 4\pi\epsilon_0 R V^2/d$ for $d \ll R$,[11] where ϵ_0 is the dielectric constant, d the distance between the sphere and the surface, and R the radius of the bead. Therefore, we can write $F=\Lambda V^2$, where $\Lambda = (1.71\pm0.01)\times10^{-10}$N/V^2 is the calibration factor obtained from the equilibrium relation $\kappa\Delta x = \Lambda V^2$, where Δx is the displacement of the cantilever once we apply a voltage V.[12] In practice, the voltage $V(t)$ is produced by an arbitrary signal generator (Agilent 33522) at 2 MHz sampling rate. The experiments were performed at a distance $d>1$ μm and for a maximum required displacement below $\Delta x = |x_f - x_i| < 3$nm. The condition $\Delta x \ll d$ is indeed very important because strictly speaking the real sphere-plane distance is $d-\Delta x$ (see Fig. 1). Thus, in principle, F is also a function of Δx. However, the condition $\Delta x \ll d$ allows us to neglect the dependence of F on x and to implement the ESE protocol, with an x independent force (see Eq. (2)). We point out that the limitations $d<R$ and $\Delta x<d$ come from the kind of forcing that we have chosen and are not imposed by the ESE. Other kinds of forcing can be used, for example, putting an electrode on the other side of the cantilever, which will not have any limitation.

The time dependent behavior of $F(t)/(\kappa x_f)$ needed to equilibrate the probe in a time t_f is obtained by inserting in Eq. (2) the experimental values of the parameters. The computed time evolutions of $F(t)$ are plotted in Fig. 1(b), for various t_f. Decreasing t_f below some threshold (for our experiment, this threshold is 0.23 ms), the behavior is no longer monotonous.

In order to emphasize the main features of ESE, we compare it to a standard step protocol (STEP) in which we instantaneously change $F(t)$ from $F_i=0$ to the final value $F_f = \kappa x_f$. In the absence of noise, the response of the system to STEP forcing obeys the equation $x(t)/x_f = 1-\exp(-\xi\omega_o t)\sin(\sqrt{1-\xi^2}\omega_o t+\phi)/\sqrt{1-\xi^2}$, where $\xi = \gamma/(2\sqrt{m\kappa})$ and $\phi = \cos^{-1}\xi$. From this time evolution, one can fix a reference velocity $v_0 = \frac{x_f}{\sqrt{1-\xi^2}}\xi\omega_o = (20.9\pm0.2)$nm/ms, which we use to compare quantitatively STEP and ESE responses.

Examples of the time evolution of $x(t)$ and $\dot{x}(t)$ for the two protocols are plotted in Fig. 2 when the equilibrium position is changed from $x_i=0$ to $x_f=0.5$ nm. In this specific illustration, we choose for ESE $t_f=2$ ms for which the needed $F(t)$ is plotted in Fig. 1(b) (blue line). In Fig. 2, we compare the STEP and ESE protocols by plotting for each of them, a single realization (blue lines) and the mean response (red lines) obtained by averaging over 5000 realizations of the protocols. Within the STEP protocol (Figs. 2(c) and 2(d)), both $x(t)$ and $\dot{x}(t)$ do not relax up to more than several τ. This has to be compared to ESE (Figs. 2(a) and 2(b)), for which the system reaches the target position x_f in the desired timelapse ($t_f=2$ ms); this is about two orders of magnitude faster than STEP. Note that the velocity scale for the velocity along ESE is five times expanded with respect to STEP. Remarkably, the ESE turns out to be very efficient even at the level of a single realization.

However, the ESE formulation put to work here cannot be operational for too small values of t_f. This can be observed by comparing results with t_f ranging from 0.2 ms to 10 ms. As shown in Fig. 3, where the ensemble averages of

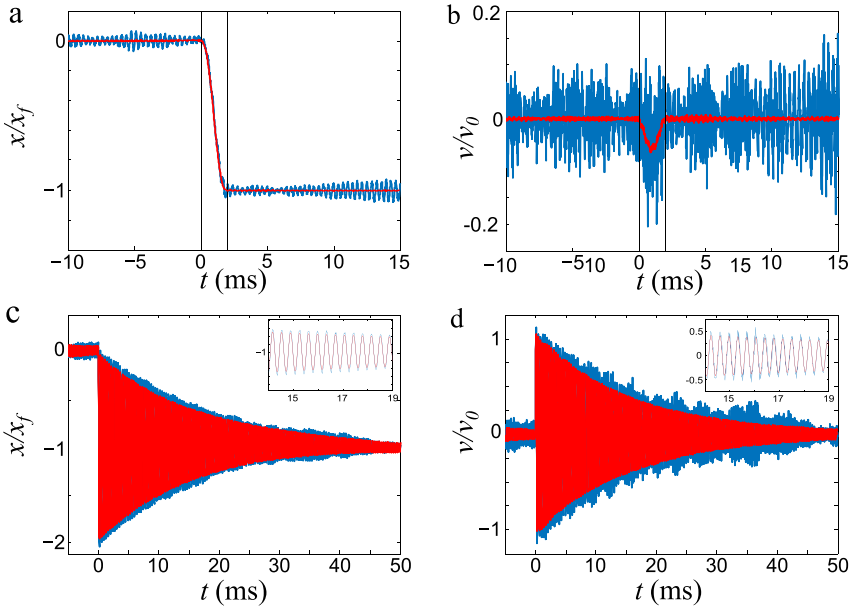

FIG. 2. Dynamics of the system along the STEP and ESE protocols. All processes start at $t=0$ ms. (a) Position evolution along the ESE process with $t_f=2.0$ ms. (b) Normalized velocity $\dot{x}(t)/v_o$ as a function of time, along the ESE process. (c) Position evolution along the STEP protocol. Intrinsic oscillations of the cantilever are much faster than the dissipation process, what makes difficult to distinguish the trajectory. The inset provides a magnification of a small region. (d) Normalized velocity evolution along the STEP process. The inset increases the time resolution, to observe the intrinsic oscillations. All figures show the dynamics of a single realization (blue) and the ensemble average over 5000 realizations (red). Vertical black solid lines in (a) and (b) represent the limits of the ESE protocol ($t_f=2$ ms).

5000 trajectories with $t_f=(0.2,\ 0.5,\ 2.0)$ ms are presented, the response of the systems to ESE protocol is excellent as long as $t_f > t_{\rm osc} = 2\pi/\omega_o \simeq 0.4$ ms. For times shorter than $t_{\rm osc}$, the ESE response remains significantly superior to its STEP counterpart, but it begins to deteriorate with the occurrence of small damped oscillations. The reason for these residual oscillations lies in the modeling of the probe dynamics. Indeed, Eq. (1) describes well the probe dynamics only for frequencies smaller than the first longitudinal mode frequency of the micromechanical oscillator. When $t_f < t_{\rm osc}$, the high order modes are also excited and Eq. (1) does not properly describe the dynamics of the tip. The effect is visible in the proper trajectory or velocity (see Fig. 3 for $t_f=0.2$ ms). However, despite this small residual error, the improvement for equilibration speed of ESE is still quite appreciable in this regime, as it can be easily checked by comparing the STEP response in Fig. 2(c) with Fig. 3(a). We emphasize that the feature addressed here is not a deficiency of the ESE method at such, but a consequence of its implementation on an equation that becomes inaccurate at a high frequency.

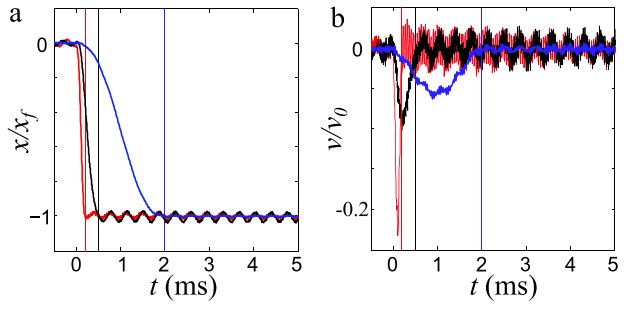

FIG. 3. Comparison of the ESE protocols at various t_f. (a) Ensemble average of the trajectory over 5000 realizations for $t_f=0.2$ ms (red), $t_f=0.5$ ms (black), and $t_f=2$ ms (blue). The higher modes start to dominate the dynamics of the system once the protocol is shorter than $2\pi/\omega_o \simeq 0.4$ ms. (b) Ensemble average of the normalized velocity for the same time periods in (a). The normalized velocity $\dot{x}(t)/v_o$ allows a better vision of the higher order effect. In both figures, the vertical lines represent the end of each protocol. All processes start at $t=0$ ms.

This is the intrinsic limitation of ESE which works as far as the mathematical model of the physical system is accurate enough.

A relevant question deals with the measurement of the energy dissipated for various values of t_f. Indeed, a good characterization of the energetics of small systems is essential to understand their time evolution, their limits, and their interactions with the environment. Even if the energy exchange is comparable with the intrinsic thermal noise, this heat release is important in small devices, either natural, such as enzymes,[13] or artificial, such as thermal nanoengines.[14] Our system has a total energy $E = U + K = \frac{1}{2}\kappa x^2 - Fx + \frac{1}{2}mv^2$, where U and K correspond to the potential and the kinetic energy, respectively. The stochastic energy received by the system along a single trajectory can be expressed as

$$\Delta E = \int_0^{t_f} \left[\frac{\partial E}{\partial F}\dot{F} + \frac{\partial E}{\partial x}\dot{x} + \frac{\partial E}{\partial v}\dot{v}\right] dt\,. \tag{3}$$

Following Ref. 15, we identify the first term in the rhs of Eq. (3) with the stochastic work δW. The heat $\delta Q = \delta E - \delta W$ splits into two contributions δQ_x and δQ_v which correspond to potential and kinetic heat, respectively.[15] The value of the dissipated heat at the end of the protocol has to correspond to the difference between the exerted work and the difference of free energy between the initial and final state $\Delta\mathcal{F}$. The free energy difference is $\Delta\mathcal{F} = \Delta U - T\Delta S_{eq}$. As the difference of the entropy of the system ΔS_{eq} between the initial and final state is zero (position-wise, the statistical distribution is simply shifted by a quantity $x_f = F_f/\kappa$) and since $\Delta E = \Delta U$ due to the isothermal condition, the free energy difference is $\Delta\mathcal{F} = \Delta U = F_f^2/2\kappa = W + Q$. In all this discussion, W and Q refer to the *mean* work and heat.

In Fig. 4, the evolution of the energetics is shown for two different ESE times, $t_f=0.2$ ms and $t_f=2$ ms. Despite the limitation of our ESE implementation for $t_f < t_{\rm osc}$, we estimate the energetics in this regime as well. Indeed, we checked that the measured time evolutions of W and Q coincide quite well with those of the numerical simulation of

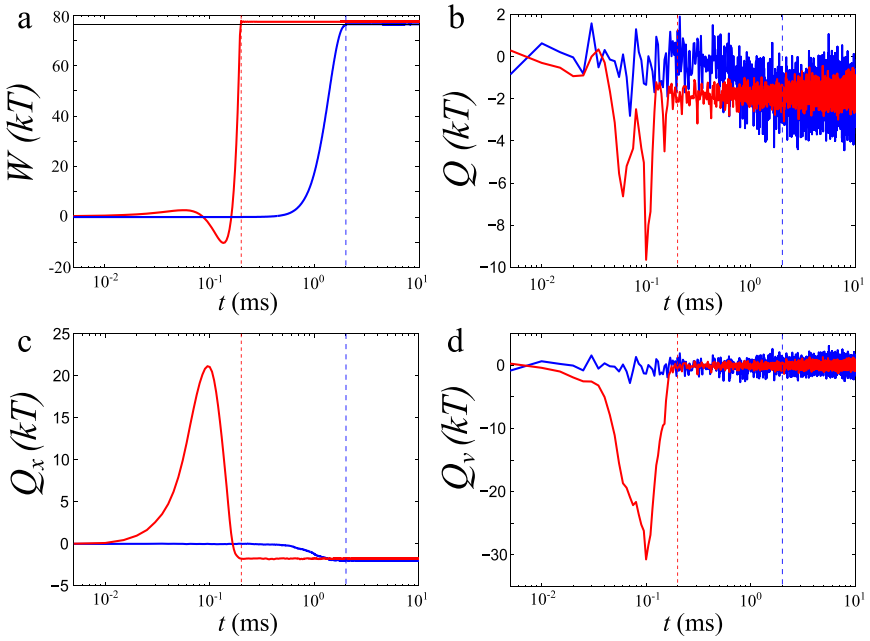

FIG. 4. Energetics of the system along the ESE route. (a) Average value of the cumulative work as a function of time for different protocol times t_f. Horizontal black line represents the difference of free energy between the initial and final state $\Delta\mathcal{F}$. (b) Average value of the cumulative total heat. (c) Average value of the cumulative potential heat. (d) Average value of the cumulative kinetic heat. Its importance reduces once we increase the protocol time. The kinetic heat is compensated with the potential one, showing the classical oscillation of a classical harmonic oscillator. In the four graphs, red lines are for $t_f = 0.2$ ms and blue lines for $t_f = 2$ ms.

Eq. (1) for the ESE protocols. This means that the residual errors remain small even when $t_f < t_{\rm osc}$, as we have shown in Fig. 3. Due to the low viscosity of the environment, dissipation lies within the detection limit of our experiment, and no significant changes are provided in the final value of the work needed to execute the protocol. However, there is a significant difference in the evolution of the energetics when t_f is larger or smaller than $t_{\rm osc}$. Indeed, we checked that for $t_f \geq 0.3$ ms the behavior of W is similar to the blue line in Fig. 4. Instead, when $t_f \leq 0.3$ ms, the protocol becomes non-monotonous to compensate for the inertial term in the dynamics (see Fig. 1(b)). Therefore, the work is not growing continuously, but becomes negative for a small time interval in the course of the transformation. This means that the system shall exercise work on the environment to ensure a relaxation on a very short amount of time. In Fig. 4(b), the total heat is plotted as a function of time. There are significant changes in the time evolution but not in the final value. The total heat is the sum of the potential and the kinetic one, shown in Figs. 4(c) and 4(d), respectively. As the cantilever moves from an equilibrium position to another rapidly, a high speed is required and a large amount of heat is absorbed via the kinetic energy. Figures 4(c) and 4(d) also show how the heat is dissipated via the potential energy and not via kinetic energy (see the nonzero value in the final times of Fig. 4(c) and the zero value in Fig. 4(d)). All graphs correspond to ensemble averages over 5000 realizations.

Using a micromechanical oscillator, we have shown that ESE protocols speed-up the relaxation time of about 2 orders of magnitude. The bound ultimately faced has to do with the limit of the modeling of the cantilever dynamics by a simple Langevin oscillator with a single resonant frequency. The ESE could be useful to design the high speed AFM, where in such a case the time t_f is the settling time needed for a fast displacement of the tip to a new position.[5] By reducing the operating time of AFM or optical trap, one enlarges the frequency window in which the system under scrutiny (biomolecule, material, and enzyme.) can be probed. Our formalism can be readily applied to the optical traps operating under vacuum and for which inertia becomes predominant.[16] We can also imagine protocols where the free parameter is the distance between the tip and the surface, modulated by a high accuracy piezoelectric device. Finally, the ESE protocols could be combined with standard feedback techniques to further decrease the operating time.

Supplementary material contains two sections. The first one describes the energy measurements are performed. The second section presents a detailed mathematical analysis on the method used to compute the ESE protocols.

This work has been supported by the ERC Contract OUTEFLUCOP. We acknowledge funding from the Investissement d'Avenir LabEx PALM program (Grant No. ANR-10-LABX-0039-PALM). We thank L. Bellon for useful discussions.

[1]C. A. Regal and K. W. Lehnert, "From cavity electromechanics to cavity optomechanics," J. Phys.: Conf. Ser. **264**, 012025 (2011).
[2]M. Hofheinz, H. Wang, M. Ansmann, R. C. Bialczak, E. Lucero, M. Neeley, A. D. O'Connell, D. Sank, J. Wenner, J. M. Martinis, and A. N. Cleland, "Synthesizing arbitrary quantum states in a superconducting resonator," Nature **459**(7246), 546 (2009).
[3]S. A. McGee, D. Meiser, C. A. Regal, K. W. Lehnert, and M. J. Holland, "Mechanical resonators for storage and transfer of electrical and optical quantum states," Phys. Rev. A **87**, 053818 (2013).
[4]A. Humphris, M. Miles, and J. Hobbs, "A mechanical microscope: High-speed atomic force microscopy," Appl. Phys. Lett. **86**(3), 34106 (2005).
[5]F. Castanié, L. Nony, S. Gauthier, and X. Bouju, "Image calculations with a numerical frequency-modulation atomic force microscope," J. Phys. Chem. C **117**, 10492–10501 (2013).
[6]S. Devasia, E. Eleftheriou, and S. O. R. Moheimani, "A survey of control issues in nanopositioning," IEEE Trans. Control Syst. Technol. **15**, 802–823 (2007).
[7]J. D. Adams, B. W. Erickson, J. Grossenbacher, J. Brugger, A. Nievergelt, and G. E. Fantner, "Harnessing the damping properties of materials for high-speed atomic force microscopy," Nat. Nanotechnol. **11**, 147–151 (2016).

[8]I. A. Martínez, A. Petrosyan, D. Guéry-Odelin, E. Trizac, and S. Ciliberto, "Engineered swift equilibration of a Brownian particle," Nature Phys. **12**, 843–846 (2016)..
[9]N. C. Singer and W. P. Seering, "Preshaping command inputs to reduce system vibrations," ASME J. Dyn. Syst., Meas., Control **112**, 76–82 (1990).
[10]P. Paolino, F. A. A. Sandoval, and L. Bellon, "Quadrature phase interferometer for high resolution force spectroscopy," Rev. Sci. Instrum. **84**(9), 095001 (2013).
[11]J. M. Crowley, "Simple expressions for force and capacitance for a conductive sphere near a conductive wall," in *Proceedings of the ESA Annual Meeting on Electrostatics 2008*, Paper No. D1, p. 1, 2008.
[12]J. R. Gomez-Solano, L. Bellon, A. Petrosyan, and S. Ciliberto, "Steady-state fluctuation relations for systems driven by an external random force," Europhys. Lett. **89**(6), 60003 (2010).
[13]C. Riedel, R. Gabizon, C. A. Wilson, K. Hamadani, K. Tsekouras, S. Marqusee, S. Pressé, and C. Bustamante, "The heat released during catalytic turnover enhances the diffusion of an enzyme," Nature **517**(7533), 227–230 (2015).
[14]I. A. Martínez, É. Roldán, L. Dinis, D. Petrov, J. M. R. Parrondo, and R. A. Rica, "Brownian Carnot engine," Nat. Phys. **12**, 67–70 (2016).
[15]K. Sekimoto, *Stochastic Energetics* (Springer, 2010), Vol. 799.
[16]T. Li, S. Kheifets, D. Medellin, and M. G. Raizen, "Measurement of the instantaneous velocity of a Brownian particle," Science **328**, 1673–1675 (2010).